WILEY InterScience®
DISCOVER SOMETHING GREAT

Exact Integration of the Stiffness Matrix of an 8-Node Plane Elastic Finite Element by Symbolic Computation

L. Videla,[1] T. Baloa,[1] D. V. Griffiths,[2] M. Cerrolaza[1]
[1] *Instituto de Materiales y Modelos Estructurales, Facultad de Ingenieria, Universidad Central de Venezuela, Caracas, Venezuela*

[2] *Colorado School of Mines, Colorado, USA*

Received 12 December 2006; accepted 4 April 2007
Published online 4 June 2007 in Wiley InterScience (www.interscience.wiley.com).
DOI 10.1002/num.20274

Computer algebra systems (CAS) are powerful tools for obtaining analytical expressions for many engineering applications in both academic and industrial environments.

CAS have been used in this paper to generate exact expressions for the stiffness matrix of an 8-node plane elastic finite element. The Maple software system was used to identify six basic formulas from which all the terms of the stiffness matrix could be obtained. The formulas are functions of the Cartesian coordinates of the corner nodes of the element, and elastic parameters Young's modulus and Poisson's ratio.

Many algebraic manipulations were performed on the formulas to optimize their efficiency. The redaction in CPU time using the exact expressions as opposed to the classical Gauss–Legendre numerical integration approach was over 50%. In an additional study of accuracy, it was shown that the numerical approach could lead to quite significant errors as compared with the exact approach, especially as element distortion was increased. Numer Methods Partial Differential Eq 24: 249–261, 2008

Keywords: exact integration; symbolic FEM manipulation; stiffness matrix; 8-node element; plane strain

I. INTRODUCTION

The finite element method (FEM) is the most popular tool for mathematical-sis of engineering and applied sciences problems in both academic and industrial environments. Generation of finite element stiffness matrices is usually carried out by numerical integration (Gaussian–Legendre quadrature) over the plane of each element. In the case of a nonlinear dynamic-sis for example, the user may be called upon to reform the element stiffness matrices for each element at each time

Correspondence to: D. V. Griffiths, Colorado School of Mines, Colorado, USA (email: d.v.griffiths@mines.edu)
Contract grant sponsor: National Science Foundation (NSF, USA); contract grant number: INT-0106665
Contract grant sponsor: Fondo Nacional de Investigaciones Científicas y Tecnológicas (FONACIT, Venezuela); contract grant number: PI-99001054

a finite element development environment based on the computer software Mathematica. The environment is used to automatically program standard element formulations and develop new elements with novel features.

Mbakogu and Pavlovi [20] discussed a variational solution obtained symbolically for the analysis of clamped plates. Also, Pavlovi [21] presented an extensive compilation on symbolic analysis of some structural engineering areas. Fields such as finite elements and variational techniques are treated using symbolic manipulation. Felippa [22] presented a set of Mathematica modules of numerical integration rules, which are then used considered for symbolic finite element work.

More recently, Lozada et al. [23] have obtained semianalytical expressions to compute the stiffness matrix of an 8-noded plane elasticity superparametric finite element. The authors reported savings of 37% in CPU times.

This work presents and discusses the exact integration of the stiffness matrix of an 8-node plane elastic superparametric finite element. The technique developed here in could be extended to other types of elements and strain conditions (i.e., axisymmetric or 3D).

II. SYMBOLIC APPROACH: FORMULATION AND IMPLEMENTATION

In what follows a brief summary of the FEM formulation for plane elasticity is included. The finite element shown in Fig. 1 is a superparametric 8-node plane elastic element, displayed in both Cartesian and local coordinate space.

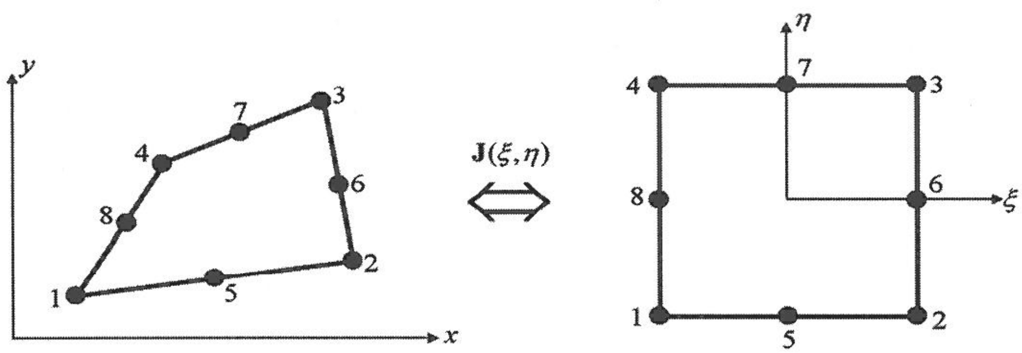

Node	Global coordinates	
	x	y
1	x_1	y_1
2	x_2	y_2
3	x_3	y_3
4	x_4	y_4
5	$(x_1+x_2)/2$	$(y_1+y_2)/2$
6	$(x_2+x_3)/2$	$(y_2+y_3)/2$
7	$(x_3+x_4)/2$	$(y_3+y_4)/2$
8	$(x_4+x_1)/2$	$(y_4+y_1)/2$

Node	Local coordinates	
	ξ	η
1	-1	-1
2	1	-1
3	1	1
4	-1	1
5	0	-1
6	1	0
7	0	1
8	-1	0

FIG. 1. 8-node plane superparametric element.

Now, a typical submatrix $\mathbf{K}_{i,j}$ is written as

$$K_{i,j} = \frac{E}{1+v}\begin{bmatrix} \displaystyle\int_{-1}^{1}\int_{-1}^{1}\frac{\frac{\partial N_i}{\partial x}\frac{\partial N_j}{\partial x}\frac{1}{(1-v)}+\frac{1}{2}\frac{\partial N_i}{\partial y}\frac{\partial N_j}{\partial y}}{|\mathbf{J}|}d\xi\, d\eta & \displaystyle\int_{-1}^{1}\int_{-1}^{1}\frac{\frac{\partial N_i}{\partial x}\frac{\partial N_j}{\partial y}\frac{v}{(1-v)}+\frac{1}{2}\frac{\partial N_i}{\partial y}\frac{\partial N_j}{\partial x}}{|\mathbf{J}|}d\xi\, d\eta \\ \displaystyle\int_{-1}^{1}\int_{-1}^{1}\frac{\frac{\partial N_i}{\partial y}\frac{\partial N_j}{\partial x}\frac{v}{(1-v)}+\frac{1}{2}\frac{\partial N_i}{\partial x}\frac{\partial N_j}{\partial y}}{|\mathbf{J}|}d\xi\, d\eta & \displaystyle\int_{-1}^{1}\int_{-1}^{1}\frac{\frac{\partial N_i}{\partial y}\frac{\partial N_j}{\partial y}\frac{v}{(1-v)}+\frac{1}{2}\frac{\partial N_i}{\partial x}\frac{\partial N_j}{\partial x}}{|\mathbf{J}|}d\xi\, d\eta \end{bmatrix} \tag{7}$$

Now, the computation of the stiffness terms of the finite element is carried out with *Maple*, by generating automatic procedures for each stiffness term. These expressions are grouped into terms having the nodal coordinates as well as the elastic parameters of the element.

Equation (7) was obtained for plane stress problems; however, the user can easily convert to plane strain conditions by replacing $\frac{1}{(1-v)}$ and $\frac{v}{(1-v)}$ by $\frac{1-v}{(2-v)}$ and $\frac{v}{(1-2v)}$ respectively.

A typical *Maple* input procedure is shown below:

```
fl:=proc(i,j,X,Y)
option inline;
DNODO[i][X]*DNODO[j][X]+DNODO[i][Y]*DNODO[j][Y]*(1/2-v/2)
end proc
```

Then, we are now able to identify six Characteristic Basic Equations (CBEs), as a function of the local coordinates ξ, η which are used to generate all the terms of the stiffness matrix. The index "i" in equation (8) stands for the number of the CBE being used ($i = 1, \ldots, 6$).

In what follows, the six CBE formulas obtained in this work are presented, as well as the stiffness matrix terms generated by each CBE. Because of the symmetry of the stiffness matrix, only 136 terms need to be calculated $(16*(16+1))/2$.

In all CBE equations, the terms $AKm(j)$, $BKm(j)$, $CKm(j)$, etc. are constants depending upon element Cartesian coordinates and elastic properties. The letter "m" indicates the number of the CBE equation ($m = 1, \ldots, 6$), while the index "j" indicates the stiffness term to be obtained. For instance, in CBE1 group, by setting $j = 1$ we will obtain $k_{1,1}$, $j = 2$ will lead to $k_{1,2}$ and so on.

In that follows, the CBEs are identified (see the Appendix for detailed expressions of CBEs):

CBE1: interaction between DOF of corner nodes

The 36 stiffness terms ($j = 1, \ldots, 36$) generated by CBE1 are

$$k_{1,1}\ k_{1,2}\ k_{1,3}\ k_{1,4}\ k_{1,5}\ k_{1,6}\ k_{1,7}\ k_{1,8}\ k_{2,2}\ k_{2,3}\ k_{2,4}\ k_{2,5}\ k_{2,6}\ k_{2,7}\ k_{2,8}\ k_{3,3}\ k_{3,4}\ k_{3,5}$$

$$k_{3,6}\ k_{3,7}\ k_{3,8}\ k_{4,4}\ k_{4,5}\ k_{4,6}\ k_{4,7}\ k_{4,8}\ k_{5,5}\ k_{5,6}\ k_{5,7}\ k_{5,8}\ k_{6,6}\ k_{6,7}\ k_{6,8}\ k_{7,7}\ k_{7,8}\ k_{8,8}$$

CBE2: interaction between DOF of corner nodes with even mid-side nodes

The 32 stiffness terms ($j = 1, \ldots, 32$) generated by CBE2 are

$$k_{1,11}\ k_{1,12}\ k_{2,11}\ k_{2,12}\ k_{3,11}\ k_{3,12}\ k_{4,11}\ k_{1,12}\ k_{5,11}\ k_{5,12}\ k_{6,11}\ k_{6,12}\ k_{7,11}\ k_{7,12}\ k_{8,11}\ k_{8,12}$$

$$k_{11,5}\ k_{11,6}\ k_{2,15}\ k_{2,16}\ k_{3,15}\ k_{3,16}\ k_{4,15}\ k_{4,16}\ k_{5,15}\ k_{5,16}\ k_{6,15}\ k_{7,15}\ k_{7,16}\ k_{8,15}\ k_{8,16}$$

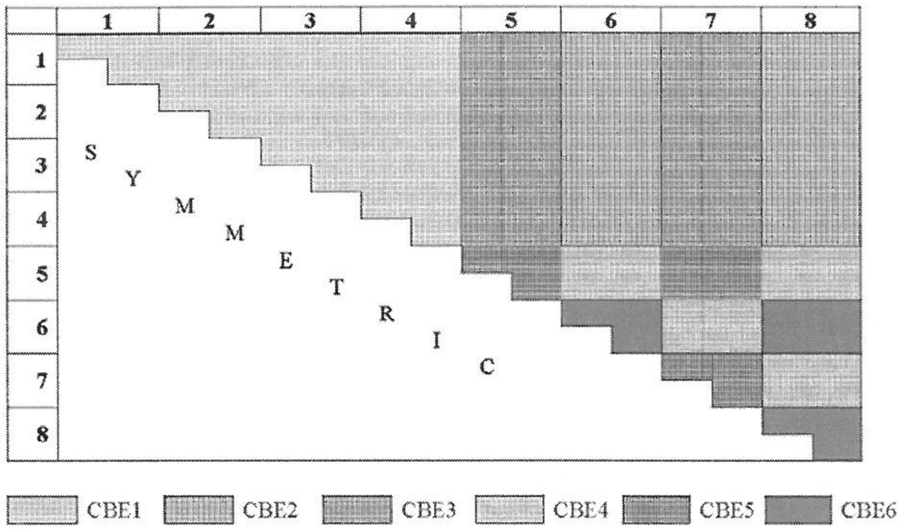

FIG. 2. Stiffness terms computed by each of the six CBEs.

of the very large size of the K, only a fraction of it is included herein:

$$\begin{aligned}K(i,j,|\mathbf{J}|) = {} & -\tfrac{1}{15} IK(i,j)CJ^4BJ^2AJ^3 + \tfrac{1}{35} DK(i,j)CJ^5BJ^2AJ^2 + \tfrac{1}{5} FK(i,j)CJBJ^4AJ^4 \\ & -\tfrac{2}{5} BK(i,j)CJ^2BJ^4AJ^3 + \tfrac{4}{105} AK(i,j)CJ^3BJ^3AJ^3 + \tfrac{1}{35} DK(i,j)CJ^3BJ^4AJ^3 \\ & -\tfrac{52}{15} BK(i,j)CJ^2BJ^6AJ - \tfrac{2}{15} BK(i,j)CJ^4BJ^4AJ + \tfrac{6}{5} HK(i,j)AJ^7CJ^2\ln(AJ+BJ+CJ) \\ & +\tfrac{1}{6} EK(i,j)AJ^7BJ^2\ln(AJ-BJ+CJ) - 2QK(i,j)AJ^6CJ^3\ln(-AJ-BJ+CJ) \\ & +\tfrac{1}{2} PK(i,j)AJ^5BJ^3CJ\ln(-AJ+BJ+CJ)\cdots \end{aligned} \tag{12}$$

The expressions obtained for each term of the stiffness matrix were optimized by simplifying and post processing the expressions. Duplicated and similar operations were deleted, as well as any other unnecessary calculations. In this way, the CPU time required to compute the stiffness terms was reduced significantly, as shown in the next section.

III. ACCURACY AND INTEGRATION TIMES

To test the accuracy and efficiency of the analytical formulations described in this paper, comparisons were made with results obtained using both 2×2 ("reduced integration") and 3×3 Gauss–Legendre quadrature. The relative error between results obtained by numerical and analytical integration was measured by using an error formula of the form:

$$\mathrm{ERROR} = \frac{\sqrt{\sum_{i,j=1}^{n}\left(K_{ij}^{\text{analytical}} - K_{ij}^{\text{numerical}}\right)}}{\sum_{i,j=1}^{n}|K_{ij}^{\text{analytical}}|} \tag{13}$$

Comparisons were made on an 8-node element, which was increasingly distorted by moving node 3, 6, and 7 (nodes 1, 2, 4, 5, and 8 are fixed) further and further away from node 1, as shown in Table I.

The limit case when the 8-node element is degenerated to a triangle yielded, as expected, singular values of the integrals.

Regarding the computation times, it can be noted that the relative error increased with element distortion CPU savings, of approximately 50% were also obtained using the analytical formulation.

Table II reports these comparisons, by considering meshes consisting of up to 1 million elements using 3×3 Gaussian rule.

Figure 3(a,b) show two cantiliver beams discretized following the McNeal–Harder Test cases [24].

A comparison of numerical results against analytical results in the McNeal-Harder test were performed and reported in Table III.

Axial and shear loading on a simple cantilever beam was analyzed, using two rather distorted elements with aspect ratios of approximately 28:1 as shown in Fig. 4.

A comparison of the displacement δ (horizontal in axial loading and vertical in shear loading) at the end of the beam by analytical integration, numerical integration, and exact beam theory is shown in Table IV.

As it can be observed in Table IV, the axial force case is integrated almost exactly by using both 2×2 and 3×3 Gaussian rules. However, in the shear force case, important numerical errors are obtained when using the 2×2 rule (25%), while the 3×3 rule leads to an error of 4.9%. Also note that, as expected, the analytical integration developed in this paper provides the same results as predicted by structural beam theory.

Two more practical engineering examples are now considered where accuracy relating to displacements and stresses by both numerical and analytical integration is compared. Figures 5

TABLE III. Comparison between analytical and numerical results corresponding to cases shown in Fig. 3.

	AXIAL			SHEAR		
CASE	$\delta_{\text{Analy}}/\delta_{(2\times2)}$	$\delta_{\text{Analy}}/\delta_{(3\times3)}$	$\delta_{\text{Analy}}/\delta_{\text{Teory}}$	$\delta_{\text{Analy}}/\delta_{(2\times2)}$	$\delta_{\text{Analy}}/\delta_{(3\times3)}$	$\delta_{\text{Analy}}/\delta_{\text{Teory}}$
Figure 3.a	1.0001	1.0000	1.0000	0.9069	0.9998	1.0000
Figure 3.b	1.0001	1.0000	1.0000	0.7114	0.9994	1.0000

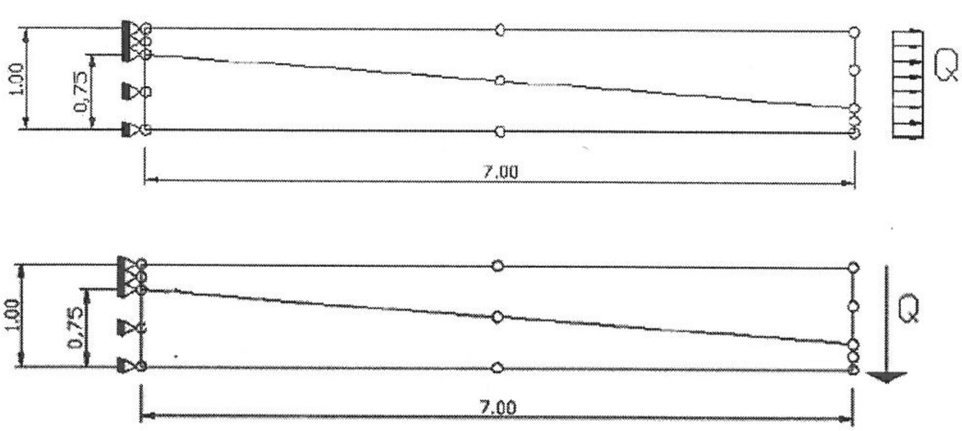

FIG. 4. Simple cantilever beam subjected to axial and shear forces.

TABLE V. Nodal displacement and element stresses comparison: numerical and analytical integration.

		2 × 2		3 × 3		4 × 4	
		Numerical	Analytical	Numerical	Analytical	Numerical	Analytical
Earth dam							
Nodal displacement	u	0.126 E − 3	0.121 E − 3	0.121 E − 3	0.121 E − 3	0.121 E − 3	0.121 E − 3
at node A	v	0.276 E − 4	0.285 E − 4	0.285 E − 4	0.285 E − 4	0.285 E − 4	0.285 E − 4
Stresses	σ_x	−0.137 E + 1	−0.124 E + 1	−0.257 E + 1	−0.222 E + 1	−0.274 E + 1	−0.274 E + 1
	σ_y	0.174 E + 1	0.196 E + 1	0.191 E + 1	0.211 E + 1	0.219 E + 1	0.219 E + 1
Quarter-plate with elliptical hole							
Nodal displacement	u	0.320 E − 1	0.308 E − 1	0.304 E − 1	0.308 E − 1	0.304 E − 1	0.308 E − 1
at node B	v	−0.786 E − 2	−0.805 E − 2	−0.804 E − 2	−0.805 E − 2	−0.804 E − 2	−0.805 E − 2
Stresses	σ_x	0.194 E + 4	0.190 E + 4	0.290 E + 4	0.293 E + 4	0.341 E + 4	0.345 E + 4
	σ_y	−0.546 E + 3	−0.469 E + 3	−0.531 E + 3	−0.589 E + 3	−0.579 E + 3	−0.580 E + 3

The same behavior is observed in element stresses at selected Gauss points, belonging to one of the elements adjacent to selected nodes (A or B).

IV. CONCLUDING REMARKS

This research was oriented towards the generation of the stiffness matrix of an 8-noded plane elasticity finite element in a fully analytical way. The main goal was to reduce substantially the integration (CPU) times, which is a subject of concern when dealing with very large FEM meshes, especially in the case of dynamic non-linear analysis. Some of the most relevant conclusions are reported below:

- Six CBEs were obtained to compute analytically the 136 stiffness terms of the 8-node plane element.
- The savings in CPU time of the order of 50%.
- The analytical integration guarantees accuracy, even for distorted elements.
- The "hand-postprocessing" of the CBEs analytical formulas generated by CAS is essential in order to reduce even more the integration times, CAS software produces well-posed formulas but many repeated operations (as well as unnecessary operations) were found in them. These operations could be removed by hand, thus improving not only the CPU time, but also leading to a reduction of the analytical code size.
- CAS software was able to output the complex analytical expressions directly into a high-level programming language, such as Fortran.

APPENDIX: CHARACTERISTIC BASIC EQUATIONS (CBEs)

CBE1: interaction between DOF of corner nodes

$$\begin{aligned}\mathrm{CBE1} = {} & ((AK1(j)\xi^2 + BK1(j)\xi + CK1(j))\eta^4 + (DK1(j)\xi^3 + EK1(j)\xi^2 + FK1(j)\xi \\ & + GK1(j))\eta^3 + (HK1(j)\xi^4 + IK1(j)\xi^3 + JK1(j)\xi^2 + KK1(j)\xi + LK1(j))\eta^2 \\ & + (MK1(j)\xi^4 + NK1(j)\xi^3 + OK1(j)\xi^2 + PK1(j)\varepsilon)\eta + (QK1(j)\xi^4 \\ & + RK1(j)\xi^3 + SK1(j)\xi^2))/|\mathbf{J}|\end{aligned}$$

3. A. R. Korncoff and S. J. Fenves, Symbolic generation generation of finite element stiffness matrices, Comput Struct 10 (1979), 119–124.
4. C. M. Andersen and A. K. Noor, A computerized symbolic integration technique for development of triangular and quadrilateral composite shallow shell finite element, Rep. NASA TN D-8067, 1975.
5. A. K. Noor and C. M. Andersen, Computerized symbolic manipulation in structural mechanics: progress and potential, Comput Struct 10 (1979), 95–118.
6. W. C. Zienkiewicz, R. L. Taylor, and J. M. Too, Reduced integration technique in general analysis of plates and shells, Int J Numer Methods Eng 3 (1971), 275–290.
7. G. Rengarajan, N. Knight, and M. Aminpour, Comparison of symbolic and numerical integration methods for an assumed-stress hybrid shell element, Commun Numer Methods Eng 11 (1995), 307–316.
8. S. Vlachoutsis, Explicit integration for three-dimensional degenerate shell finite element, Int J Numer Methods Eng 29 (1990), 861–880.
9. G. Yagawa, G. W. Ye, and S. Yoshimura, A numerical integration scheme for finite element method based on symbolic manipulation, Int J Numer Methods Eng 29 (1990), 1539–1549.
10. N. S. Bardel, The application of symbolic to computing to the hierarchical finite element method, Int J Numer Methods Eng 28 (1989), 1181–1204.
11. A. Mizukami, Some integration formulas for a four-noded isoparametric element, Computat Methods Appl Mech Eng 59 (1986), 111–121.
12. M. Kikuchi, Application of the symbolic mathematics system to the finite element program, Comput Mech 5 (1989), 41–47.
13. H. D. Rathod, Some analytical integration formulae for a four node isoparametric element, Comput Struct 30 (1988), 1101–1109.
14. D. V. Griffiths, Stiffness matrix of the four-node quadrilateral element in closed form, Int J Numer Methods Eng 37 (1994), 1027–1038.
15. J.-P. Cardoso, Generation of finite element matrices using computer algebra, Masters Thesis, School of Engineering, University of Manchester, UK, 1994.
16. D. V. Griffiths and I. M. Smith, Programming the finite element method, 4th Ed., Wiley, 2004.
17. L. Videla, N. Aparicio, and M. Cerrolaza, Explicit integration of the stiffness matrix of a four-noded-plane elasticity finite element, Commun Numer Methods Eng 12 (1996), 721–743.
18. J. Korelc, Automatic generation of finite-element code by simultaneous optimization of expressions, Theor Comput Sci 187 (1997), 231–248.
19. K. Y. Chee, J. T. Boyle, and D. A. Mackenzie, A computer algebra based finite element environment, Adv Eng Softw 32 (2001), 913–925.
20. F. C. Mbakogu and M. N. Pavlovi, Bending of clamped orthotropic rectangular plates: a variational symbolic solution, Comput Struct 77 (2000), 117–128.
21. M. N. Pavlovi, Symbolic computation in structural engineering, Comput Struct 81 (2003), 2121–2136.
22. C. A. Felippa, A compendium of FEM integration formulas for symbolic work, Eng Comput 21 (2004), 867–890.
23. I. J. Lozada, J. C. Osorio, D. V. Griffiths, and M. Cerrolaza, Semi-analytical integration of the 8-node plane element stiffness matrix using symbolic, J Numer Methods Partial Differential Equations 22 (2006), 296–316.
24. R. MacNeal and R. L. Harder, A proposed set of problems to test finite element accuracy, J Finite Element Anal Des 1 (1985), 3–20.